Minimally Invasive Arthroscopy for Achilles Tendinopathy

11

Yu-jie Liu, Feng Qu, and Hai-peng Li

11.1 Introduction

The Achilles tendon, the most powerful tendon in the human body that carries and transmits the body's load, is formed by the joint of the gastrocnemius and soleus tendons and attached to the calcaneal tuberosity (Fig. 11.1) [1, 2]. Achilles tendinopathy may be associated with exercise overload, repeated accumulation of chronic fatigue injury, resulting in chronic damage to Achilles tendon fibers [3].

In the literature, 24.0–45.5% of Achilles tendinitis is reported, which is refractory to conservative treatment [4]. Conventionally, we use of open surgery for calcification cleaning, radiofrequency ablation, bone protrusion (Haglund's nodule) resection, and fixation of Achilles tendon insertion. The author designed and carried out radiofrequency ablation, debridement, and osteophyte grinding under arthroscopic surveillance to treat this disease in 2004 and received satisfactory clinical efficacy, which avoids tissue scarring and blood supply damage to the peritendinous tissue after open surgery [5] and is beneficial for lesion healing and early functional rehabilitation.

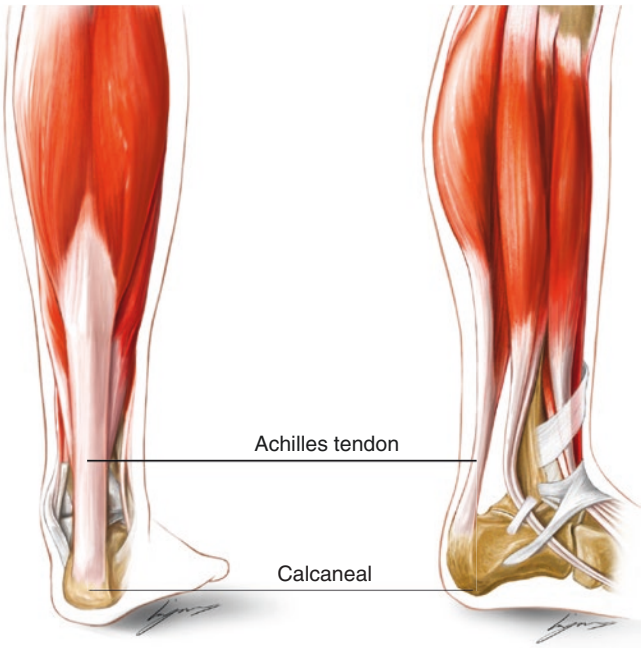

Fig. 11.1 Gross anatomy of Achilles tendon

11.2 Clinical Features

Plain radiographs show hyperostosis of the calcaneal tuberosity (Fig. 11.2) with calcification in the Achilles tendon (Fig. 11.3); CT displays worm-like changes in the calcaneal tuberosity (Fig. 11.4); and MRI exhibits mixed signals in the

Fig. 11.2 Hyperostosis of calcaneal tuberosity under plain X-ray

Y.-j. Liu (✉)
Department of Orthopedics, Chinese PLA General Hospital, Beijing, China

F. Qu
Beijing Tongren Hospital, Capital Medical University, Beijing, China

H.-p. Li
Department of Orthopedics, The 7th Medical Center of Chinese PLA General Hospital, Beijing, China

Y.-j. Liu et al. (eds.), *Advanced Application of Arthroscopy*, https://doi.org/10.1007/978-981-15-4684-6_11

Fig. 11.3 Hyperplastic calcified shadow at Achilles tendon attachment

Achilles tendon (Fig. 11.5) [6]. Ultrasonography disclosed partial rupture of Achilles tendon fibers and abnormal echo area of bursa and peritendinous tissue.

11.2.1 Clinical Typing

Achilles tendinopathy is classified into calcific tuberosity (Fig. 11.6), fibrous tear (Fig. 11.7), hypertrophic hypertrophy (Fig. 11.8), and calcaneal tuberosity hyperplasia (Haglund's deformity, Fig. 11.9) based on clinical, radiographic, and arthroscopic findings [7].

11.3 Preoperative Preparation

Prepare a 30° diameter 2.7-mm-wide angle arthroscope, radiofrequency plasma knife generator and timer, TOPAZ radiofrequency electrode blade (Fig. 11.10). The Achilles tendon anatomical outline, pain points, and surgical portals (Fig. 11.11) are marked preoperatively; and local infiltration anesthesia was performed with 2% lidocaine around the lesion and in the surgical approach (Fig. 11.12). A 10-mm

Fig. 11.4 Cortex of calcaneus at the attachment of Achilles tendon with worm-like changes by CT

lateral opening is made 20 mm proximal to the Achilles tendon pain point to create an arthroscopic and an instrument pathway (Fig. 11.13) [8]. Operative procedures were performed under arthroscopic surveillance.

11.4 Operative Technique

11.4.1 Calcified Nodular Type

Most of the patients suffered sudden onset, severe pain, sometimes at night, and could not be touched locally. X-rays

Fig. 11.5 Mixed signals in the Achilles tendon under MRI

Fig. 11.7 Achilles tendon fiber tear type

Fig. 11.6 Calcified nodule type

Fig. 11.8 Hyperplastic fertilizer

Fig. 11.9 Hyperplastic type of calcaneal tuberosity (Haglund's deformity)

Fig. 11.10 TOPAZ electrode blades

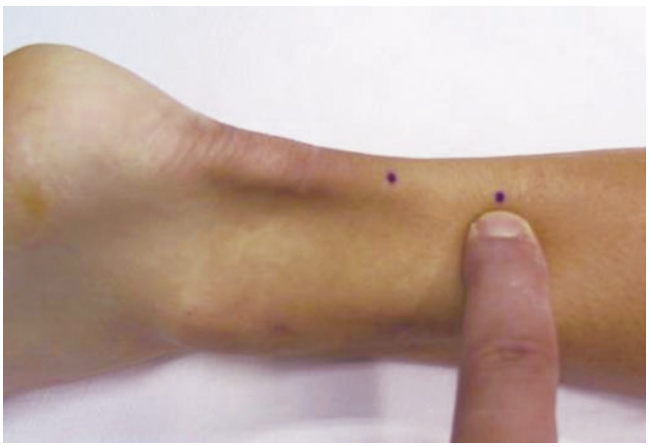

Fig. 11.11 Anatomical outline, pain points, and surgical approach of Achilles tendon marked before operation

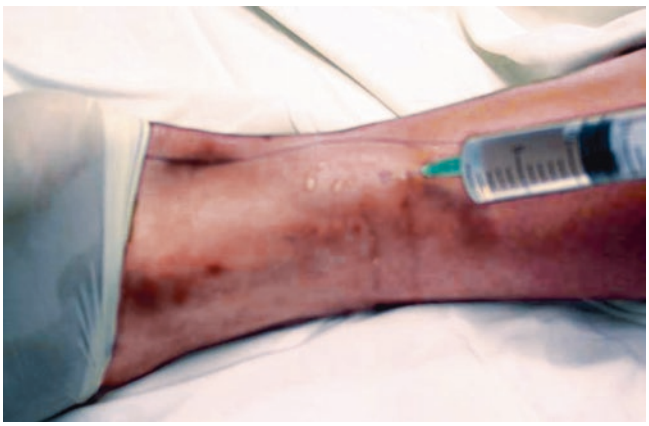

Fig. 11.12 Local infiltration anesthesia around lesion and surgical approach with 2% lidocaine

Fig. 11.13 A 10 mm lateral to both sides of Achilles tendon 20 mm proximal to lesion for arthroscopic and surgical access

display increased density of calcified shadows attached to the calcaneal tuberosity (Fig. 11.14), and MRI presents strip hyperintense calcifications in the Achilles tendon (Fig. 11.15). Arthroscopic exploration of the aponeurosis revealed rose-red hyperemia and edema (Fig. 11.16). The deep layer of the opened aponeurosis is a whitish lime-like slag of calcification (Fig. 11.17), and the calcified material is similar to calcified supraspinatus tendinitis of the shoulder.

After arthroscopic shaver cleaning, flush the released calcification with a large volume of saline. The edge of the calcified Achilles tendon lesion is then cleaned with a plasma knife (Fig. 11.18). The pain symptoms can be significantly relieved after the calcium material is cleaned. Immobilization was performed with a plaster cast or ankle brace for 3 weeks after surgery to allow healing of the injured Achilles tendon fibrous tissue and aid in functional rehabilitation.

Fig. 11.14 Calcified shadows of increased density in Achilles tendon at attachment of calcaneal tuberosity under X-rays

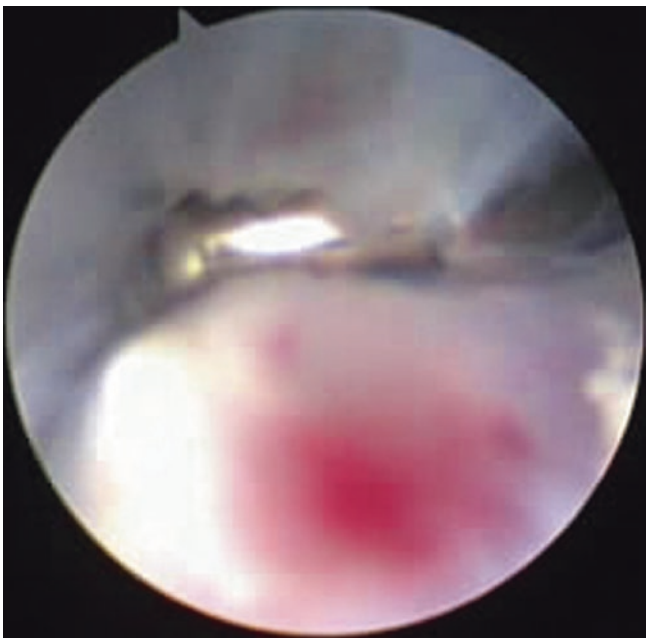

Fig. 11.16 Rose-red hyperemic area on surface of aponeurosis arthroscopy

Fig. 11.15 Striped hyperintense calcified signal in Achilles tendon tissue under MRI

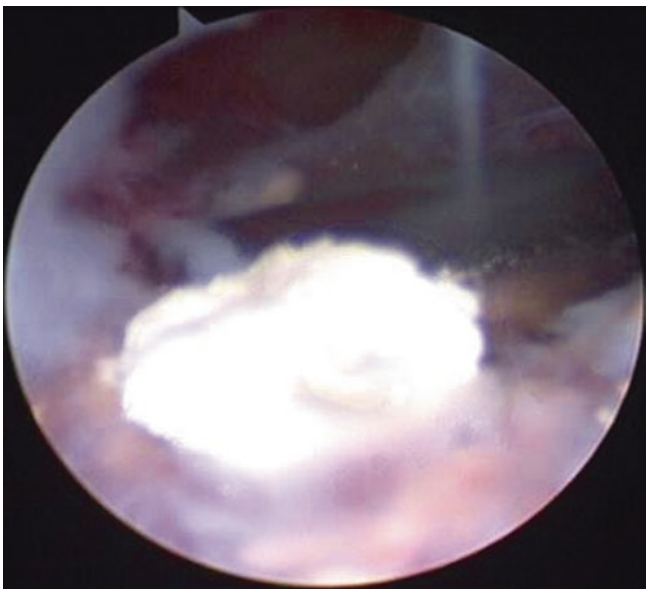

Fig. 11.17 Calcified substance with white lime slag in Achilles tendon

11.4.2 Fiber Tear Type

This type is mostly triggered by sports injury, which occurs in the middle third of the Achilles tendon, and there is no obvious positive manifestation on X-ray and CT scan. MRI may reveal structural derangements of the Achilles tendon tissue as high signal intensity (Fig. 11.19). Arthroscopic exploration reveals loss of Achilles tendon lustre, curling fibrous tissue, and disorganized structures (Fig. 11.20), partial rupture of Achilles tendon fibrous tissue defects (Fig. 11.21), and with deep continuity. Under the surveillance of arthroscope, shaver was used to clean up the broken, rough, and curly fiber and hypertrophic scar tissue. Radiofrequency ablation (Fig. 11.22) is followed by immobilization in a cast or brace for 3–4 weeks.

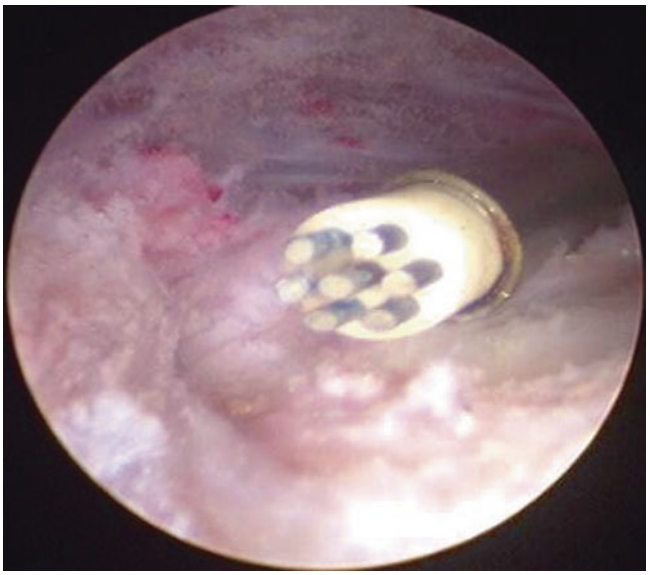

Fig. 11.18 Plasmakinetic debridement of calcified Achilles tendon edge

Fig. 11.19 Disordered structure of Achilles tendon fiber tear and tissue edema under MRI

11.4.3 Hypertrophic Type

Lesions occurred mainly in the tissues where the calcaneal tuberosity was attached to the Achilles tendon. Rough cracked skin with hyperpigmentation and hyper-

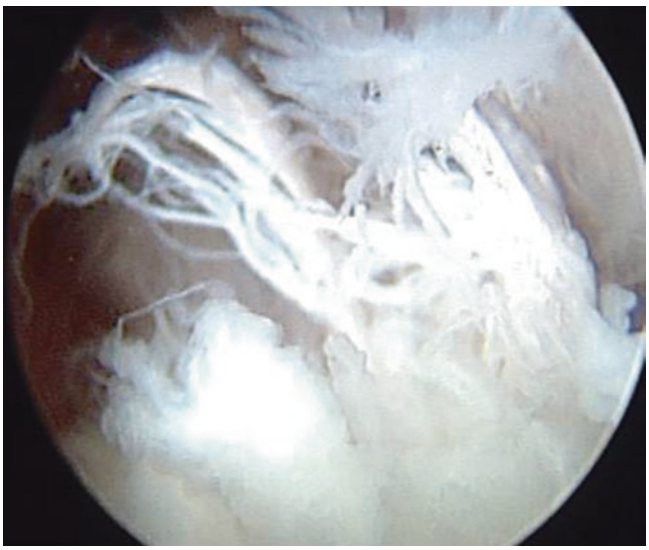

Fig. 11.20 Partial disruption of Achilles tendon tissue with curled fibers and disorganized structure under arthroscopic exploration

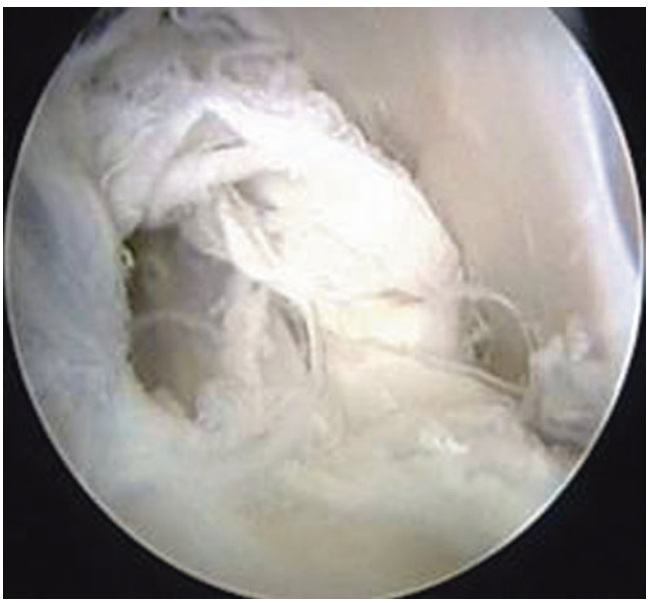

Fig. 11.21 Partial rupture and defect of fibrous tissue of Achilles tendon

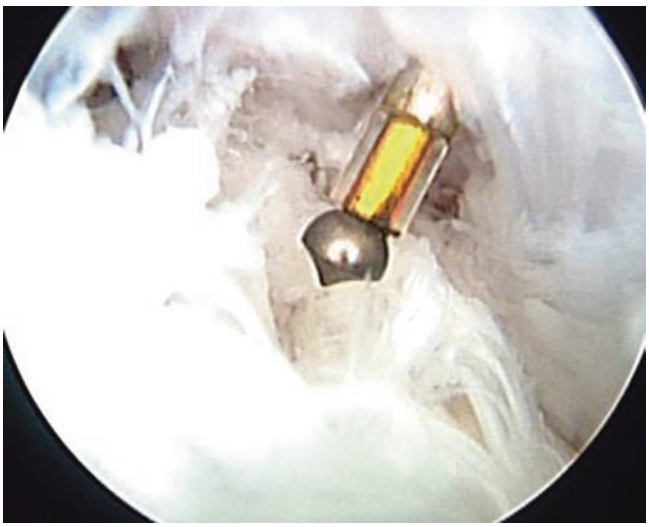

Fig. 11.22 Radiofrequency ablation technique

Fig. 11.23 Clinical manifestations of heel swelling, soft tissue hyperplasia and hypertrophy around calcaneal tuberosity

trophy around the calcaneal tuberosity are the clinical findings (Fig. 11.23). X-rays and CT scans show hyperostosis or worm-like changes in the calcaneal tuberosity (see Fig. 11.4). MRI demonstrates abnormal signal intensity in the Achilles tendon disorganization (Fig. 11.24) with

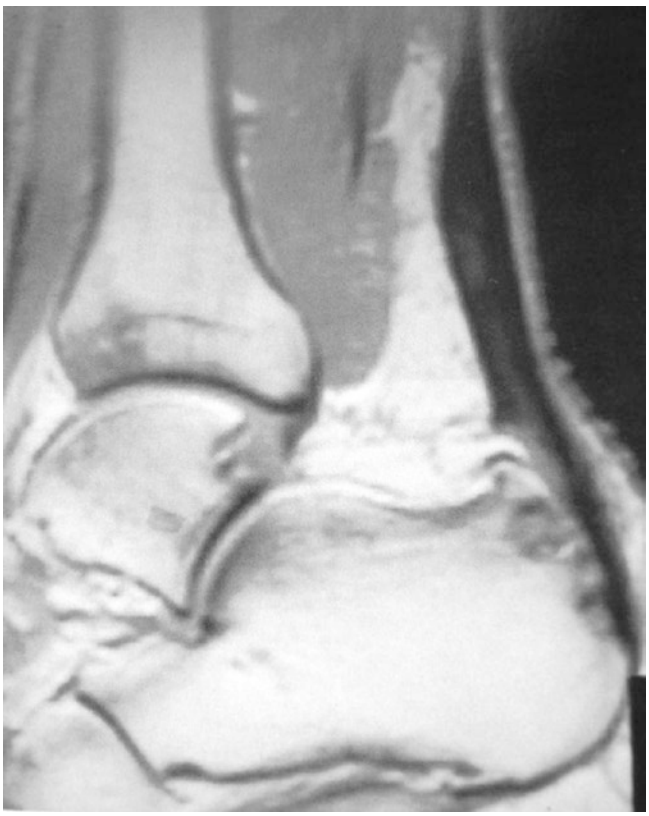

Fig. 11.24 Worm-like changed and signal abnormal Achilles tendon at the attachment of the calcaneal tuberosity under MRI

worm-like changes at the calcaneal tuberosity. Arthroscopic exploration reveals disorganized tissue at the calcaneal tuberosity Achilles tendon attachment (Fig. 11.25) and fibrous disruption and scar hyperplasia in some Achilles tendons (Fig. 11.26).

Fibrous scar tissue on the surface of Achilles tendon is cleaned by arthroscopy (Fig. 11.27). Radiofrequency ablation is performed at the attachment of Achilles tendon using TOPAZ (Fig. 11.28). It is vertically inserted into the deep layer of Achilles tendon to reach the calcaneal tuberosity with a treatment point at 3 mm interval. The treatment time is 0.5 s at each point, with pressure 5–8 g. The appearance of lesion area after treatment is mesh-like (Fig. 11.29) [9]. The incision of 3 mm was sutureless, externally dressed, and immobilized for 3 weeks with an ankle brace. Functional rehabilitation training was carried out gradually after operation. The swelling of the Achilles tendon tissue at the calcaneal tuberosity subsides by 6 weeks (Fig. 11.30).

11.4.4 Calcaneal Tubercle Hyperplasia (Haglund's Deformity)

Haglund's anomaly is defined as an abnormal protrusion of the posterosuperior calcaneal tubercle, accompanied by inflammation around the insertion of the Achilles tendon,

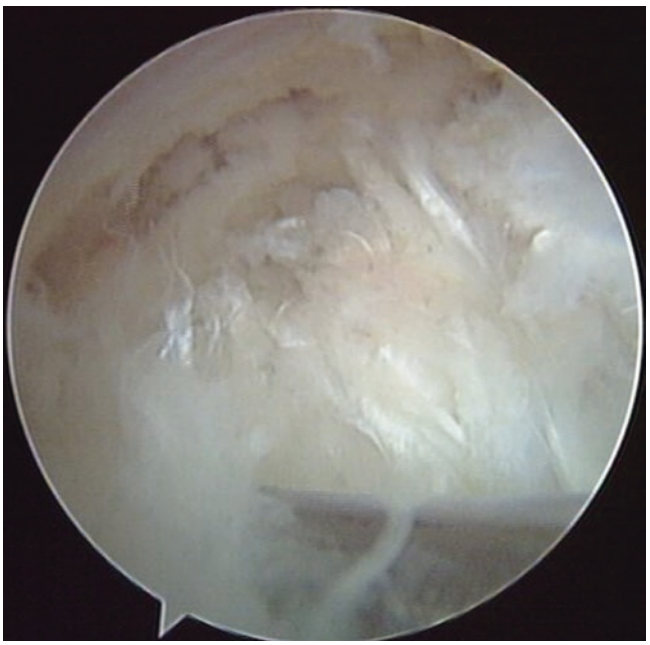

Fig. 11.25 Disorganized tissue at calcaneal tuberosity Achilles tendon attachment under arthroscopic exploration

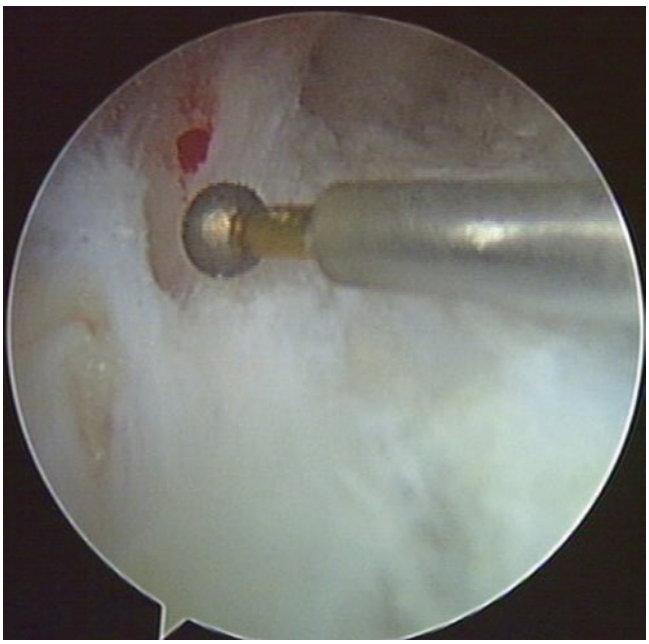

Fig. 11.27 Arthroscopic debridement of hypertrophic fibrous scar tissue of Achilles tendon

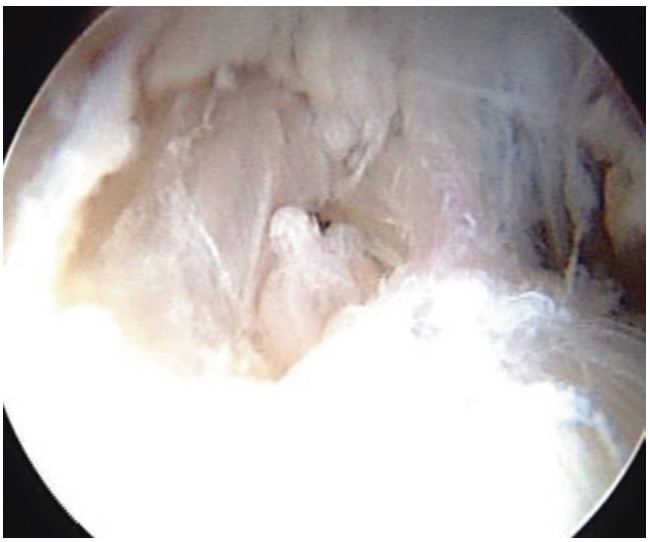

Fig. 11.26 Partial fracture and scar hyperplasia of Achilles tendon fibrous tissue

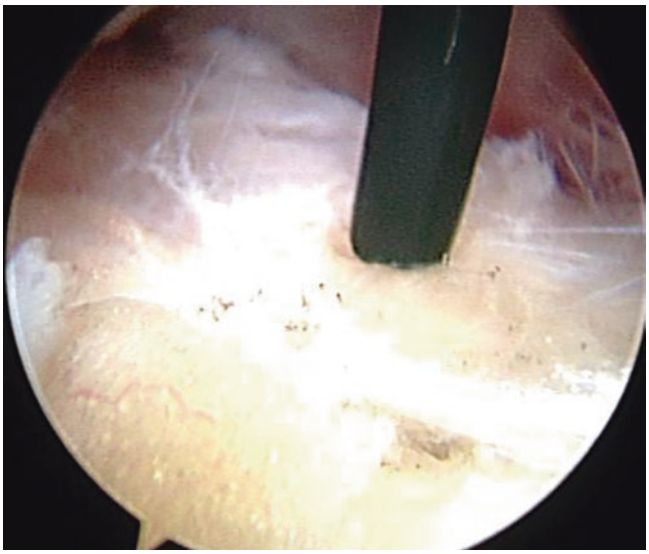

Fig. 11.28 TOPAZ radiofrequency ablation with vertical penetration into calcaneal tuberosity

and is a type of Achilles tendinopathy. The clinical manifestations were swelling and tenderness behind the Achilles tendon and limitation of dorsal extension of the foot. CT examination showed the superior posterior process of the calcaneus. MRI presented congestion and edema of the Achilles tendon.

The patient was placed in a prone position with the foot and ankle positioned distally to facilitate intraoperative passive ankle mobilization (Fig. 11.31). The distal end of the medial and lateral malleoli and the medial and lateral edges of the Achilles tendon were marked, and the posterior and posterior medial approaches were used for arthroscopic treatment of Haglund's deformity. The posterior arthroscopic approach was routinely selected slightly higher than the calcaneus.

Fig. 11.29 Topical mesh after TOPAZ radiofrequency ablation

Fig. 11.30 Rough swelling skin of right heel before treatment and swelling around calcaneal tuberosity subsided 6 weeks after operation

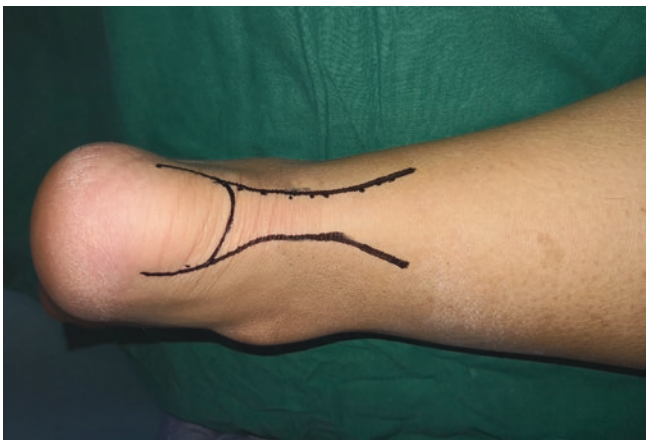

Fig. 11.31 Surgical position

The posterolateral surgical approach is first established, the skin is incised with a sharp knife and then punctured with a blunt tip awl and a cannula directed toward the posterosuperior calcaneal tubercle, and a 4 mm diameter, 30° angled arthroscope is inserted. The posterior internal approach is established under arthroscopic surveillance by first puncturing with a syringe needle to confirm proper position and angle, incising the skin 3 mm, and then separating the lacuna from the adipose tissue beneath the Achilles tendon (Fig. 11.32). After filling with water, a shaver blade is placed to clean the adipose tissue beneath the Achilles tendon, fully exposing the Achilles tendon, the Achilles tendon bursa, and the posterior bursa mucosa and superior anapophysis of the calcaneus (Fig. 11.33). The hyperemic bursa in front of the Achilles tendon was cleaned, and the ankle joint was moved passively to observe the impact of the posterior superior calcaneal tubercle and the Achilles tendon. Insert the needle of the syringe behind the Achilles tendon to the posterior superior tuberosity of the calcaneus under arthroscopic surveillance (Fig. 11.34), locate fluoroscopically to identify the area of osteophyte removal from the calcaneus (Fig. 11.35), abrade the osteophyte portion (Fig. 11.36), and perform a negative impact test and hind-

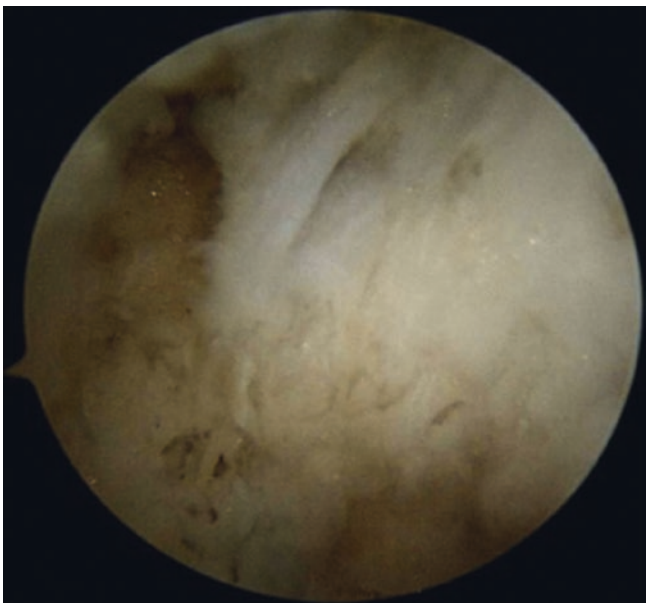

Fig. 11.32 Peel the posterior malleolus to create operating cavity

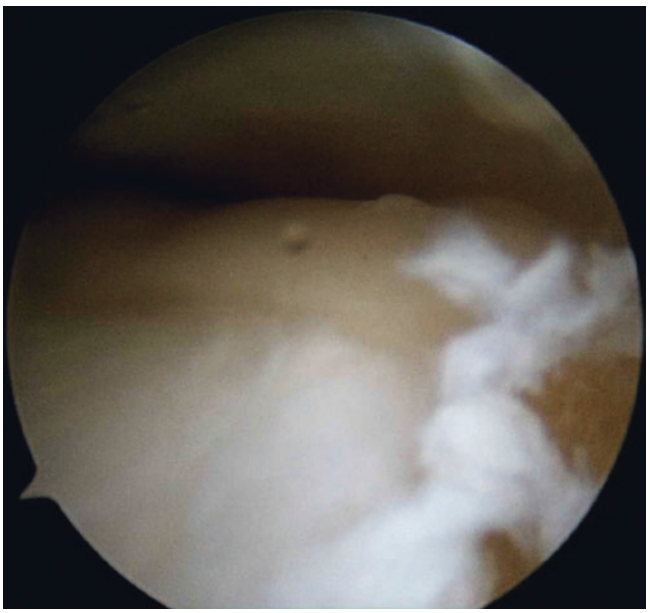

Fig. 11.34 Confirm the position of posterosuperior calcaneal tubercle under arthroscopic surveillance

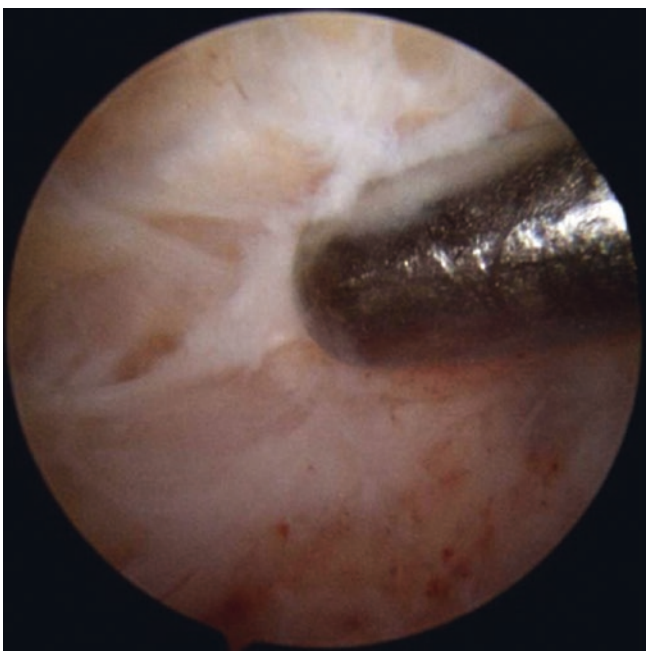

Fig. 11.33 Shaver debridement to expose Achilles tendon, Achilles bursa, and poster superior calcaneal process

Fig. 11.35 Location of the posterosuperior calcaneal tubercle under fluoroscopy

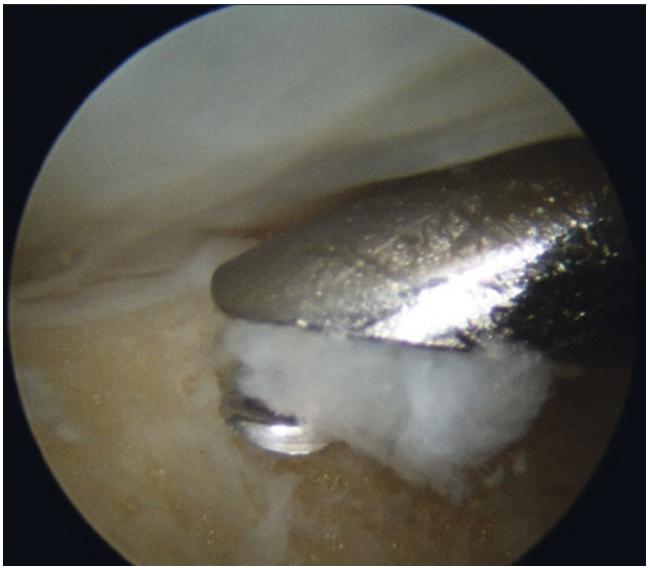

Fig. 11.36 Grinding and drilling to remove part of posterosuperior tuberosity of calcaneus

Fig. 11.37 Posterior superior calcaneal tuberoplasty

foot varus impact test (Fig. 11.37). Lesions in the superficial layers of the Achilles tendon were also managed in parallel. Note residual osteophytes at the posterolateral or posteromedial approach to the posterior superior calcaneal tuberoplasty (Fig. 11.38), resulting in residual postoperative symptoms [10].

Fig. 11.38 Residual osteophytes under CT 3D reconstruction

11.5 Critical Points

1. Imaging studies such as MRI are important for the preoperative diagnosis of Achilles tendinopathy and the development of treatment options.
2. Haglund's deformity preoperative 3D CT can show the extent and location of the bony prominence, facilitating the removal of the lesion during surgery.
3. Patients who frequently undergo local hormonal blockade are prone to Achilles tendon rupture or non-healing wounds.
4. Achilles tendon fiber tear pattern due to reduced strength of the Achilles tendon tissue, 4–6 weeks after surgery should be developed to prevent rupture.

References

1. Silva RT, et al. Medical assistance at the Brazilian juniors tennis circuita one-year prospective study. J Sci Med Sport. 2003;6:14–8.
2. Jarde O, et al. Surgical treatment of chronic Achilles tendiopathies: report of 52 cases. Rev Chir Orthop Reparatrice Appar Mot. 2000;86:718–23.
3. Thermann H, Benetos IS, Panelli C, Gavritlidis I, Feil S. Endoscopic treatment of chronic mid-portion Achilles tendinopathy: novel technique with short-term results. Knee Surg Sports Traumatol Arthrosc. 2009;17(10):1264–9.

4. Maquirriain J, Ayerza M, Costa Paz M, Muscolo DL. Endoscopic surgery in chronic achilles tendinopathies: a preliminary report. Arthroscopy. 2002;18(3):298–303.
5. Ahmed IM, Lagopoulos M, McConnell P, et al. Blood supply of the achilles tendon. J Orthop Res. 1998;16:591–6.
6. Maquirriain J. Endoscopic surgery in chronic achilles tendinopathies: a preliminary report. Arthroscopy. 2002;18:298.
7. Yu-Jie L, Zhi-Gang W, Zhong-Li L, et al. Arthroscopically assisted radiofrequency probe to treat achilles tendinitis. Chin J Surg. 2008;46(2):101–3.
8. McAllister JE, Hyer CF. Safety of Achilles detachment and reattachment using a standard midline approach to insertional enthesophytes. J Foot Ankle Surg. 2015;54(2):214–9.
9. James P, Tasto JP, Cummings J, Medlock V, Hardesty R, Amiel D. Microtenotomy using a radiofrequency probe to treat lateral epicondylitis. Arthroscopy. 2005;21:851–60.
10. Roth KE, Mueller R, Schwand E, et al. Open versus endoscopic bone resection of the dorsolateral calcaneal edge: a cadaveric analysis comparing three dimensional CT scans. J Foot Ankle Res. 2014;7(1):56.